Submitted to Proc. 26th Int. Conf. of the Physics of Semiconductors, Edinburgh, 2002

Resonant spin-orbit interactions and phonon spin relaxation rates in superlattices

J A Majewski and P Vogl

Walter Schottky Institute and Physics Department, Technische Universität München, Am Coulombwall 3, D-85748 Garching, Germany

Abstract. We present band structure studies, based on first-principles and tight-binding calculations, of the zero field spin splitting energies in conduction bands of superlattices and heterostructures. We find that the spin relaxation and spin precession of conduction electrons in nanostructures can be tailored to a much larger extent than has been hitherto assumed. In wide quantum wells, we predict the k-linear spin splitting energy in the conduction band to have a pronounced angular anisotropy as a function of the applied electric field, in contrast to what envelope function theory suggests. Even in unbiased common-atom heterostructures, the spin splitting can be resonantly enhanced due to band crossings or zero-gap situations by at least one order of magnitude. In no-common-atom heterostructures, the microscopic interface asymmetry is found to dominate the spin splitting, irrespective of any applied electric field. In addition, we show that acoustic and optic phonons lead to spin-flip processes and we present quantitative results for the spin-phonon deformation potentials in GaAs.

1. Introduction

The present surge in interest for spin devices and spin relaxation effects calls for a detailed understanding of the spin dynamics in semiconductor nanostructures [1]. We will focus on [001] grown zincblende structures in this paper, where the spin-split energies in the conduction bands may be considered as the result of an effective lateral **k**-dependent magnetic field. This field induces a coherent spin precession of incoming electrons which is counteracted by incoherent spin-independent and spin-dependent scattering events [2-5]. These spin-related effects have been studied extensively both theoretically [6-13] and experimentally [14-18], yet there are still many open questions concerning the microscopic origin of the spin-splitting of the energy bands, their dependence on material combinations, on quantum well widths of heterostructures, and on electric fields.

In this paper we attempt to answer some of these questions by first-principles, relativistic local density calculations, augmented by empirical tight-binding studies. We find that a fine-tuned band-structure engineering allows one to tailor the spin precession frequency of conduction electrons in nanostructures by very significant amounts. In addition, we present calculations of the acoustic and optic spin-phonon deformation potentials that contribute to the incoherent spin relaxation.

Zincblende heterostructures or superlattices with a [001] growth axis possess a symmetry that leads to a Mexican-hat-type structure of the conduction band edge near the Γ-point. This is a consequence of a **k**-linear spin splitting of the conduction band states of the form [9]

$$\Delta E_{\uparrow\downarrow} = 2k_{//}\sqrt{(\alpha_{BIA}^2 + \alpha_{SIA}^2) - 2\alpha_{BIA}\alpha_{SIA}\sin(2\theta)}, \quad (1)$$

where the lateral wave vector perpendicular to the growth axis is given by $k_x = k_{//}\cos\theta, k_y = k_{//}\sin\theta$. For structures that possess tetragonal D_{2d} symmetry, only the so-called bulk inversion asymmetry (BIA) coupling α_{BIA} (see, e.g., [8]) is nonzero. In systems of lower C_{2v} symmetry that support a polar axis (such as asymmetric quantum wells or no-common-atom superlattices), the so-called structure inversion asymmetry (SIA) or Rashba term (see, e.g., [19]) α_{SIA} leads to an angular modulation in the spin-splitting energy. In bulk zincblende materials, there are no **k**-linear terms in the conduction band at the Γ-point.

In heterostructures, these spin-orbit related coupling constants for electrons have been studied mostly in the framework of envelope function theory so far [6-13]. In its simplest form, **k•p** theory predicts the following properties of α_{BIA} and α_{SIA} for the conduction band:

(i) The BIA term is given by $\alpha_{BIA} = \gamma < k_z^2 >$, where γ is the bulk Dresselhaus constant [20] and the average is taken over the zone-center wave function. Consequently, $\alpha_{BIA} \propto L^{-2}$ decreases rapidly with the width of a quantum well.

(ii) The SIA term vanishes for a symmetric unbiased quantum well of type A:B:A, independent of the type of materials A and B.

(iii) An external electric field F along the growth axis does not change the BIA coupling, whereas the SIA term increases in proportion to it. Together with item (i), this leads to the wide-spread assumption [6-13] that the SIA term dominates in long quantum channels.

In this paper, we provide both quantitative and qualitative results that show that all of these limitations can be overcome and both α_{BIA} and α_{SIA} can be tailored independently even in wide quantum well structures.

2. Theoretical methods and physical origin of k-linear spin splitting

We have employed the local density functional method (LDA) that we have implemented with fully relativistic pseudopotentials [21]. This method reproduces the experimentally known zone-center split-off energies Δ_0 in the valence band of bulk semiconductors very accurately. In order to be able to study the relativistic electronic structure of mesoscopic heterostructures, we have carefully augmented this first-principles approach by an sp^3s^*-tight-binding model including the spin-orbit interaction. Throughout this work, we have employed the LDA framework for the study of superlattices consisting of less than 60 atomic layers and used the tight-binding method for larger structures. The results agree very well with one another for small heterostructure widths. We focus in this paper on the spin splitting energies of the lowest conduction band in zincblende nanostructures and will discuss valence band properties elsewhere.

Apart from the quantitative results, the first-principles calculations provide a global understanding of the physical origin of the **k**-dependent spin splitting energies. Qualitatively, our findings may be explained in a tight binding picture which will be substantiated by the detailed results that follow below. Since the conduction states of, say, GaAs are derived from atomic s-states, their intra-atomic spin-orbit interaction vanishes. However, the atomic Ga s-states interact with their neighboring As p-states via a hopping matrix element $t_{sp\sigma}$. For *p*-states, the intra-atomic spin-orbit interaction is non-zero. Therefore, the Ga-s states possess an indirect inter-atomic spin-orbit interaction by coupling to their neighboring p-states. It is second order in $t_{sp\sigma}$ and leads to a spin-splitting of the conduction band that is proportional to $\Delta_{SO}(t_{sp\sigma}/E_{gap})^2 k_{//}^n$ where Δ_{SO} is the intra-atomic spin-orbit interaction on the As-site and the power *n* depends on the symmetry of the entire structure. Thus, the magnitude of the conduction band spin-splitting scales inversely with the square of the energy gap which agrees well with previous first-principles and experimental chemical trends for the Dresselhaus constant γ [20]. The energy gap E_{gap} in the expression above need not be the fundamental energy gap; as we will show below, any kind of band crossing leads to a resonant enhancement of the spin splitting.

3. SIA-terms in no-common-atom superlattices

A symmetric heterostructure A:B:A possesses a nonzero SIA coupling if the materials A and B share no common atom since the interface asymmetry destroys the D_{2d} symmetry in such a case [16]. We have carried out LDA calculations of $(InP)_n$:$(AlSb)_m$ and $(InP)_n$:$(GaAs)_m$ short-period superlattices and compared them to common-atom $(AlAs)_n$:$(GaAs)_m$ superlattices for various values of n and m. We find, for example, α_{SIA} = 0.112 eVÅ and α_{SIA} = 0.043 eVÅ for the first conduction band of the $(InP)_3$:$(AlSb)_3$ and $(InP)_3$:$(GaAs)_3$ superlattices, respectively. Detailed studies lead us to conclude that the SIA coupling is primarily determined by the *wave-function asymmetry* within the quantum well layers but is insensitive to the spin-orbit interaction at the interface or within the barrier layers. The BIA constants are given by α_{BIA} = 0.034 eVÅ, α_{BIA} = 0.064 eVÅ, α_{BIA} = 0.052 eVÅ, for $(AlAs)_3$:$(GaAs)_3$, $(AlSb)_3$:$(InP)_3$, and $(InP)_3$:$(GaAs)_3$, respectively, thus having the same order of magnitude for all of these superlattices.

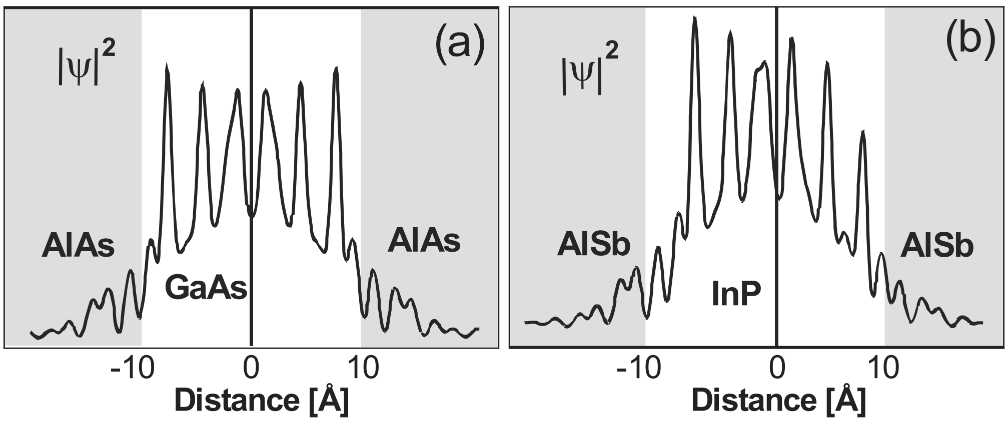

Figure 1. The laterally averaged square of the zone center conduction band wave function in (a) common-atom $(AlAs)_3(GaAs)_3$, and (b) no-common-atom $(AlSb)_3(InP)_3$ superlattices. Note that the sequence of atoms across the AlAs/GaAs structure is Al-As-Ga-...-Ga-As-Al and therefore mirror-symmetric, in contrast to the AlSb/InP superlattice with Sb-Al-Sb-$(In\text{-}P)_n$-Al-Sb that is not mirror-symmetric for any integer *n*.

In Fig. 1 we show a comparison of the square of the laterally averaged electronic wave function of the lowest conduction band at the Γ-point of a common-atom

$(AlAs)_3$:$(GaAs)_3$ and no-common atom $(AlSb)_3$:$(InP)_3$ superlattice, respectively. The asymmetry in the wave function throughout the quantum well region in the latter case is clearly seen.

4. BIA-terms in AlAs:GaAs:AlAs heterostructures

We have studied the spin-splitting of the lowest as well as higher conduction bands at $\mathbf{k}_{//} = 0$ for AlAs:$(GaAs)_n$:AlAs heterostructures as a function of the number n of GaAs layers, up to values of $n = 100$ which corresponds to a quantum well-width of approximately 30 nm. As shown in Fig. 2, the BIA constant for the first conduction band decreases with increasing n or, equivalently, with the well width L. In contrast to simple envelope function theory, however, we find this decrease to be given by $\alpha_{BIA} \propto L^{-1}$ and thus to be much slower than the anticipated L^{-2} decrease. Most importantly, the calculations show that the second and third conduction band cross each other for a value of $n \sim 20$ which leads to a resonant enhancement of the BIA-coupling *by more than one order of magnitude*. While this crossing of higher conduction bands (which occurs due to back-folding effects of the band structure along the growth axis) may be difficult to utilize in a device, we have found similar resonant enhancements due to band crossings close to the conduction and valence band edges that can be induced either by uniaxial strain, by a suitable heterostructure well width, or a combination of both effects. Thus, band structure engineering allows one to grossly enhance the spin splitting which is favorable for applications where a fast spin precession is required.

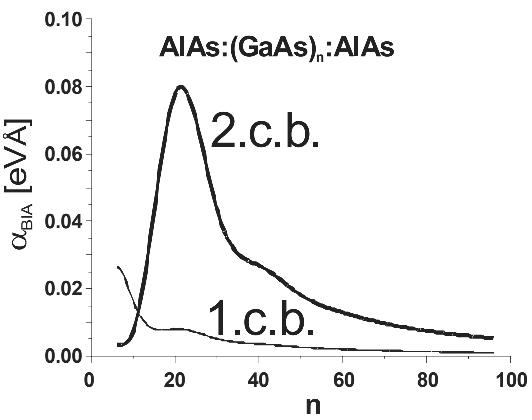

Figure 2. Calculated BIA constants (in eVÅ) for the first (1.c.b.) and second (2.c.b.) conduction band as a function of the number of GaAs layers n in AlAs:$(GaAs)_n$:AlAs heterostructures.

5. Field dependence of BIA and SIA-terms in AlAs:(GaAs)n:AlAs heterostructures

Any reduction of the D_{2d} symmetry by an applied electric field or by an asymmetric strain in common-atom heterostructures leads to a finite SIA coupling in principle. We show here that an applied electric field affects both BIA and SIA terms in an unexpected way. We study common-atom AlAs:$(GaAs)_n$: AlAs heterostructures as a function of n and assume that an applied potential drops linearly within the GaAs well region but remains zero in the (doped) barrier regions.

In Fig. 3 we show the calculated BIA- and SIA-coupling associated with the lowest conduction band edge for up to $n = 100$ GaAs layers and for three different electric fields F. For narrow heterostructures, α_{BIA} is seen to be independent of F in accord with simple envelope function theory. For the wider wells, however, the potential drop reaches almost 1 eV which is smaller than but of the order of the band width of the lowest conduction band. This leads to a localization of the conduction band wave function in real space that is shown in Fig. 3 for the various field values and for the case $n = 50$. Correspondingly, it becomes delocalized and a superposition of many band states in **k**-space. This is a situation that clearly goes beyond simple effective mass theory. As a consequence, we find this distorted wave function to lead to a BIA coupling that increases approximately linearly with the electric field and saturates for long well widths. This saturation can easily be understood: for a given field value F, the wave function is localized in one portion of the quantum well region and does not feel a prolongation of the well in the opposite direction. The SIA coupling shows exactly the same trend as the BIA coupling but reaches a *smaller* value for wide wells and the highest fields considered (see Fig. 3).

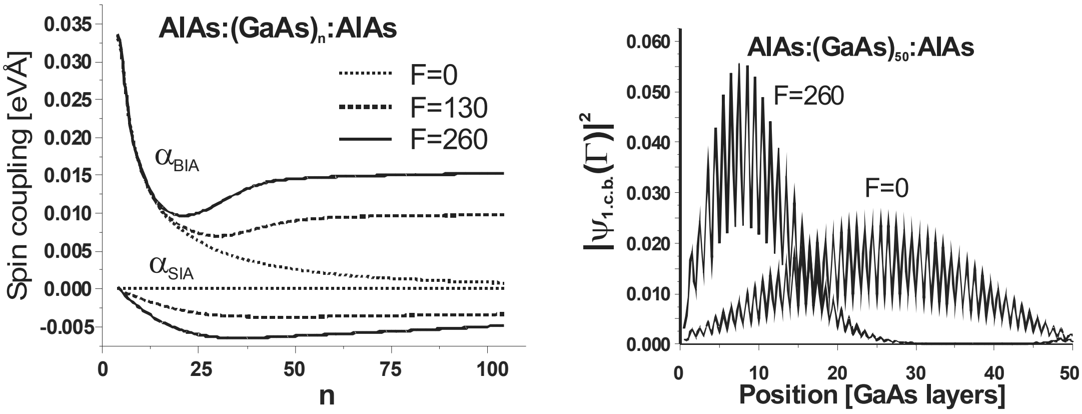

Figure 3. (a) Calculated BIA and SIA constant of the conduction band in AlAs:$(GaAs)_n$:AlAs heterostructures as a function of the number of GaAs layers n for various values of the constant electric field (in kV/cm) that is applied across the GaAs quantum well. (b) Square of the laterally averaged conduction band wave function at the Γ-point in AlAs:$(GaAs)_{50}$:AlAs for different values of external electric field (in kV/cm).

6. Higher-order spin-splittings

Most experiments that have been used to analyze spin-splitting so far are based on SdH measurements in doped structures [14, 18]. For an accurate control of the spin precession of carriers injected into a [001] heterostructure, it is essential to ensure that the spin splitting is nearly constant in some region of lateral $(k_x, k_y) = k_{//}(\cos\theta, \sin\theta)$-space that is probed by the injected carriers. This is the case when the spin-splitting is dominated by the **k**-linear terms alone. Unfortunately, this holds for a tiny portion of the Brillouin Zone only; higher order terms lead to rapid angular variations in the spin splitting of the conduction band. These processes eventually destroy the spin coherence. To show this quantitatively, we have calculated the conduction band edge spin-splitting as a function of the angle θ and for values of $k_{//}$ from 10^{-3} Å^{-1} to $2\text{x}10^{-2}$ Å^{-1} for an AlAs:$(GaAs)_{50}$:$Ga_{0.7}Al_{0.3}As$ asymmetric heterostructure. Since it possesses only C_{2v}-symmetry, it shows a weak SIA effect in addition to the dominant BIA coupling.

In Fig. 4, one can see that the angular variation of the spin splitting that is determined by Eq. (1) for the smallest wave vector ($k = 10^{-3}$ Å^{-1}), becomes a rapidly varying function already for k-values that amount to less than 2% of the Brillouin Zone. These oscillations are caused by k^3- and higher order terms in the spin splitting.

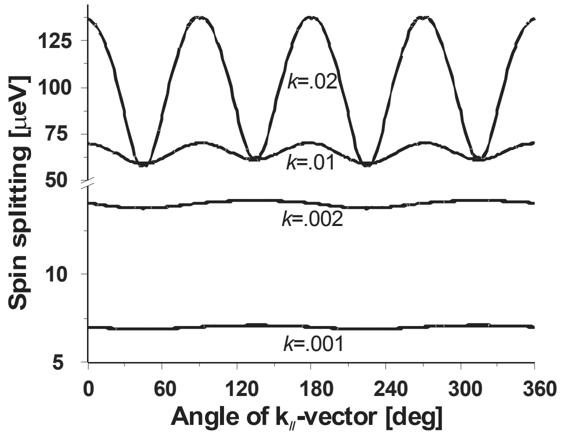

Figure 4. Spin splitting energy of the conduction band in the asymmetric AlAs:$(GaAs)_{50}$:$Ga_{0.7}Al_{0.3}As$ heterostructure as a function of the lateral **k**-vector $\mathbf{k} = k_{//}(\cos\theta, \sin\theta)$ near the zone center as a function of the angle θ and for the indicated magnitudes $k_{//}$ (in units Å^{-1}).

7. Spin-phonon deformation potentials

We show in this section that the spin-flip electron scattering by acoustic and optic phonons in zincblende bulk materials is determined by *phonon induced BIA and SIA coupling constants*. We present concrete numerical results for GaAs. In the unstrained material, only the light- and heavy-hole bands show a (tiny) **k**-linear spin splitting of the form $\varepsilon = \pm C\{k^2 \pm [3(k_x^2 k_y^2 + \text{c.p.})]^{1/2}\}^{1/2}$. The present *ab-initio* calculations give C = 0.0049 eVÅ, in reasonable agreement with previous calculations [22, 23]. Elastic or phonon deformations of the bulk crystal, on the other hand, induce a much larger linear k-splitting in the conduction band.

A tetragonal strain reduces the T_d symmetry to D_{2d} and leads to a BIA effect in the conduction band of the form $\alpha_{BIA} = B(\varepsilon_{xx} - \varepsilon_{zz})$ that is first order in the strain. We find the acoustic spin-phonon deformation potential to be given by B = 0.245 eVÅ for the conduction band. An even larger value of 2.94 eVÅ is obtained for the split-off band. We note that the higher-order **k**-terms have an angular dependence of the form $\Delta E_{\uparrow\downarrow} = 2\alpha_{BIA}k_{//} + k_{//}^3(A\cos^2\theta + B\sin^2\theta)$ [24], which differs from the bulk Dresselhaus terms.

A frozen zone-center optical phonon, characterized by a relative shift $au/4$ of the 2 sublattices, leads to a uniaxial C_{2v} symmetry and therefore induces a SIA term in the conduction band that is first order in u. In addition, a BIA term is induced that is second order in u. Thus, the optical one-phonon spin deformation potential is determined by a SIA coupling, whereas the two-phonon spin deformation potential is determined by a BIA term. We find (in eVÅ) $\alpha_{SIA} = -4.12u$ and $\alpha_{BIA} = 135.3u^2$ for the conduction band. Both constants decrease strongly with volume, $d\ln\alpha_{SIA}/d\ln V = 10.6$ and $d\ln\alpha_{BIA}/d\ln V = 9.6$, which originates in the increase of the energy gap in a compressed crystal. This further substantiates the qualitative picture of the origin of the spin splitting given in Sec. 2.

In summary, we have presented full band structure studies of the zero field spin splitting energies in semiconductor heterostructures. In symmetric unbiased common-atom structures, the spin splitting is determined entirely by bulk inversion asymmetry (BIA) terms which generally decrease with increasing well width but can be resonantly enhanced due to band crossings or zero-gap situations. The BIA term increases considerably in proportion to an applied electric field in quantum wells of a width larger than approximately 5nm, in contrast to the published predictions of envelope-function theory [7, 9-11, 13]. In no-common-atom heterostructures, the microscopic interface asymmetry induces a large structure inversion asymmetry or Rashba constant.

Financial support by the Deutsche Forschungsgemeinschaft and by the Office of Naval Research under Contract No. N00014-01-1-0242 is gratefully acknowledged.

References

[1] Prinz G A 1999 Science 283 330
[2] D'yakonov M I and Perel' V I 1971 Fiz. Tverd. Tela 13 3581 [1972 Sov. Phys. Solid State 13 3023]
[3] D'yakonov M I and Kachorovskii V Yu 1986 Fiz. Tekh. Poluprovodn. 20 178 [1986 Sov. Phys. Semicond. 20 110]
[4] Averkiev N S, Golub L E and Willander M 2002 J. Phys.: Condens. Matter 14 R1-R13
[5] Lau W H, Olesberg J T and Flatté M E 2001 Phys. Rev. B 64 161301
[6] D'yakonov M I and Perel' V I 1984 Optical Orientation Eds Meier F and Zakharchenya B P (Amsterdam: North-Holland) p 11
[7] Pikus G E and Titkov A N 1984 Optical Orientation Eds Meier F and Zakharchenya B P (Amsterdam: North-Holland) p 11
[8] Pfeffer P and Zawadzki W 1995 Phys. Rev. B 52 R14332
[9] de Andrada e Silva E A 1992 Phys. Rev. B 46 1921
[10] Eppenga R and Schuurmans M F H 1988 Phys. Rev. B 37 10923
[11] Wissinger L, Rössler U, Winkler R, Jusserand B and D Richards 1998 Phys. Rev. B 58 15375
[12] Santos P V, Willatzen M and Cardona M 1995 Phys. Rev. B 51 5121
[13] de Andrada e Silva E A, La Rocca G C and Bassani F 1997 Phys. Rev. B 55 16293
[14] Das B, Datta S and Reifenberger R 1990 Phys. Rev. B 41 8278
[15] Grundler D 2000 Phys. Rev. Lett. 84 6074
[16] Olesberger J T, Lau W H, Flatté M E, Yu C, Altunkaya E, Shaw E M, Hasenberg T C and Boggess T F 2001 Phys. Rev. B 64 201301
[17] Rowe A C H, Nehls J and Stradling R A 2001 Phys. Rev. B 63 201307 and references cited therein
[18] Jusserand B, Richards D, Peric H and Etienne B 1992 Phys. Rev. Lett. 69 848
[19] Bychkov Y A and Rashba E I 1984 J. Phys. C 17 6039; Rashba E I 1960 Fiz. Tverd. Tela 2 1224 [1960 Sov. Phys. Solid State 2 1109]
[20] Cardona M, Christensen N E and Fasol G 1988 Phys. Rev. B 38 1806
[21] Hemstreet L A, Fong C Y and Nelson J S 1993 Phys. Rev. B 47 4238
[22] Surh M P, Li Ming-Fu and Louie S G 1991 Phys. Rev. B 43 4286

[23] Cardona M, Christensen N E and Fasol G 1986 Phys. Rev. Lett. 56 2831
[24] von Allmen Paul 1992 Phys. Rev. B 46 15382